



Cite this: *RSC Sustainability*, 2024, **2**, 2949

## Magnetic polyvinylpolypyrrolidone polymer composite-supported copper(I) catalyst: an efficient and easily reusable catalyst for sustainable synthesis of 1,2,3-triazoles in water<sup>†‡</sup>

Noura Aflak,<sup>a</sup> Fatima-Ezzahraa Essebbar,<sup>b</sup> Lahoucine Bahsis,<sup>b</sup> Hicham Ben El Ayouchia,<sup>b</sup> Hafid Anane,<sup>b</sup> Miguel Julve<sup>c</sup> and Salah-Eddine Stiriba<sup>b</sup>

The development of sustainable products and processes involves the use of green chemistry principles. A new and facile synthesis of a recoverable copper(I) catalyst supported on magnetic crosslinked polyvinylpolypyrrolidone ( $\text{Fe}_3\text{O}_4$ -PVPP) for the synthesis of 1,2,3-triazole derivatives under copper-catalyzed azide–alkyne cycloaddition reactions (CuAAC) is presented in this study. The magnetic support was prepared by *in situ* co-precipitation of  $\text{Fe}_3\text{O}_4$  in polyvinylpolypyrrolidone followed by immobilization of copper(I) on the magnetic support to afford a Cu(I)/PVPP- $\text{Fe}_3\text{O}_4$  composite, which was characterized using several techniques. Its catalytic efficiency in CuAAC working under low copper catalyst loading leads to the selective synthesis of 1,4-disubstituted-1,2,3-triazoles with good to excellent yields. The green aspect of this catalytic process relies on using water as catalytic reaction medium, working at room temperature, easy isolation of 1,2,3-triazoles and simple separation of the composite catalyst by exposure to an external magnet for recovery and further reuse. The greenness of the procedure was also assessed through the atom economy (AE), E-factor and EcoScale, showing low waste generation and better sustainability scores.

Received 10th June 2024  
Accepted 13th August 2024

DOI: 10.1039/d4su00292j

rsc.li/rscsus

### Sustainability spotlight

Given recent environmental requirements, developing sustainable chemical processes is crucial. This study focuses on the copper-catalyzed Huisgen cycloaddition reaction (CuAAC) within click chemistry by heterogenizing the catalytically active copper(I) species using a biocompatible magnetite polymer ( $\text{Fe}_3\text{O}_4$ -PVPP). The resulting Cu(I)-PVPP- $\text{Fe}_3\text{O}_4$  composite enables regioselective formation of 1,2,3-triazoles in excellent yields using water as a benign solvent. This method eliminates the need for additives like reducing agents or bases and operates under environmentally friendly conditions at room temperature. Demonstrating good green chemistry metrics, including atom economy, E-factor, and EcoScale parameters, this work also aligns with the UN SDGs by promoting environmentally benign, resource-efficient, and innovative chemical processes that support responsible consumption (SDG 12) and industrial innovation (SDG 9).

## Introduction

1,2,3-Triazoles are important organic compounds that are widely applied in biology, pharmaceuticals, medicine, and

materials science.<sup>1</sup> One of the commonly used strategies reported for the synthesis of 1,2,3-triazole derivatives is the azide–alkyne 1,3-dipolar cycloaddition reaction.<sup>2</sup> This reaction was first established and carried out by Huisgen<sup>2</sup> at high temperatures in organic solvents affording a mixture of 1,4- and 1,5-regioisomers of 1,2,3-triazoles.<sup>2</sup> Within the context of the development of click chemistry reactions; Sharpless<sup>3,4</sup> and Meldal<sup>5</sup> independently reported the use of copper(I) in the Huisgen 1,3-dipolar cycloaddition reaction, leading to the regioselective formation of 1,4-disubstituted-1,2,3-triazoles under mild reaction conditions. This process, known as the copper-catalyzed azide–alkyne cycloaddition (CuAAC) reaction, has been distinguished with two Nobel Prizes. Since its discovery, CuAAC has been intensively studied under both homo- and heterogeneous regimes in view of promoting strict click chemistry conditions and sustainable processes.<sup>6–11</sup> Recent efforts on CuAAC have focused on the development of

<sup>a</sup>Département de Chimie, Faculté des Sciences d’Agadir, Université Ibn Zohr, 80000 Agadir, Morocco. E-mail: [noura.aflak@gmail.com](mailto:noura.aflak@gmail.com)

<sup>b</sup>Laboratoire de Chimie Analytique et Moléculaire/LCAM, Faculté Polydisciplinaire de Safi, Université Cadi Ayyad, 46030 Safi, Morocco. E-mail: [stiriba@uv.es](mailto:stiriba@uv.es)

<sup>c</sup>Instituto de Ciencia Molecular/ICMol, Universidad de Valencia, C/Catedrático José Beltrán 2, 46980 Valencia, Spain

<sup>†</sup> In memory of Professor Miguel Julve, who passed away on 9 July 2024. Everyone who knew him will forever remember this outstanding scientist and true gentleman.

<sup>‡</sup> Electronic supplementary information (ESI) available: Comparative study of the catalytic activity of Cu(I)/PVPP- $\text{Fe}_3\text{O}_4$  with other heterogenous copper-based catalysts, kinetic data of the CuAAC and the characterization data of the 1,2,3-triazole products (3a–3k). See DOI: <https://doi.org/10.1039/d4su00292j>



heterogeneous catalytic systems to improve the catalyst recovery, reduction of metal contamination in the final triazole products, and enhancement of the overall sustainability of the process. These advancements include the use of supported copper nanoparticles, magnetic catalysts, and polymer-based supports, which have led to promising results in terms of efficiency and eco-friendly aspects of CuAAC reactions.<sup>12–17</sup>

In recent years, the introduction of magnetic supports in catalysis has attracted great interest, firstly because of the effortless separation of the magnetic support from the reaction mixture by means of an external magnet<sup>18,19</sup> and secondly, the magnetic separation proves to be a highly efficient and practical technique for catalyst recycling when compared to conventional methods like filtration and centrifugation.<sup>20,21</sup> In general, the magnetic catalysts are constructed from functionalized magnetic nanoparticles by organic ligands and their immobilization on solid supports enhances the recyclability of the catalysts being used.<sup>21–23</sup> Different solid matrices have been employed as materials of this type, such as graphene oxide, carbon, and polymers.<sup>24</sup> Although the most suitable solid will always depend on the future application of the material, organic polymers have often been a suitable choice because of their high processability and versatility.<sup>25</sup> Moreover, the *in situ* precipitation of magnetic nanoparticles within a polymeric matrix stands as an exceptional technique for crafting magnetic polymers. This approach boasts advantages such as straightforward processing, cost-effectiveness, minimal toxicity, flexibility, stability, recyclability, and an environmentally friendly profile. These qualities collectively render the use of magnetic polymer-supported catalysts a compelling substitute for traditional reagents. Furthermore, the application of magnetic polymer-supported catalysts has garnered considerable attention due to its ability to simplify the purification of the reaction products and also to offer enhanced selectivity, both being undeniably appealing aspects of this methodology.<sup>26</sup>

The crosslinked polyvinylpolypyrrolidone (PVPP) is an insoluble polymeric backbone featuring good biocompatibility and thermal stability, unlike polyvinylpyrrolidone (PVP), which is water-soluble. The use of PVPP as insoluble support for catalysts in organic reactions has been barely addressed.<sup>26–28</sup> In this context, we have recently reported the stabilization of copper nanoparticles in PVPP and the employment of the resulting composite (CuNPs-PVPP) in a series of heterogenous CuAAC reactions.<sup>27–30</sup> The CuNPs-PVPP system efficiently catalyzes the azide–alkyne cycloaddition reactions as well as one-pot

three three-component reactions to afford 1,2,3-triazoles in water at room temperature. Its recovery by filtration and reuse was also demonstrated. Having in mind these results, we now investigate a new approach to obtain easily separable and reusable heterogenous CuAAC by direct immobilization of copper(i) catalyst on magnetic crosslinked PVPP, noted as Cu(i)-PVPP-Fe<sub>3</sub>O<sub>4</sub>. The synthesized Cu(i)-PVPP-Fe<sub>3</sub>O<sub>4</sub> composites were then applied to a series of azide–alkyne 1,3-dipolar cycloaddition reactions under click chemistry conditions, using water as the solvent and working at room temperature, fulfilling with the green chemistry principles. The prepared composite catalyst was studied in terms of reuse and recyclability as well as in the greenness of the catalytic process.

## Results and discussion

### Synthesis and characterization of Cu(i)/PVPP-Fe<sub>3</sub>O<sub>4</sub> composites

The synthesis of Cu(i)/PVPP-Fe<sub>3</sub>O<sub>4</sub> nanocomposites was carried out in two steps as outlined in Scheme 1. Firstly, the magnetic polymer (PVPP-Fe<sub>3</sub>O<sub>4</sub>) was synthesized using the *in situ* chemical co-precipitation method. In the second step, copper(i) ions have been immobilized on the magnetic support by the impregnation method. The final structure of the resulting

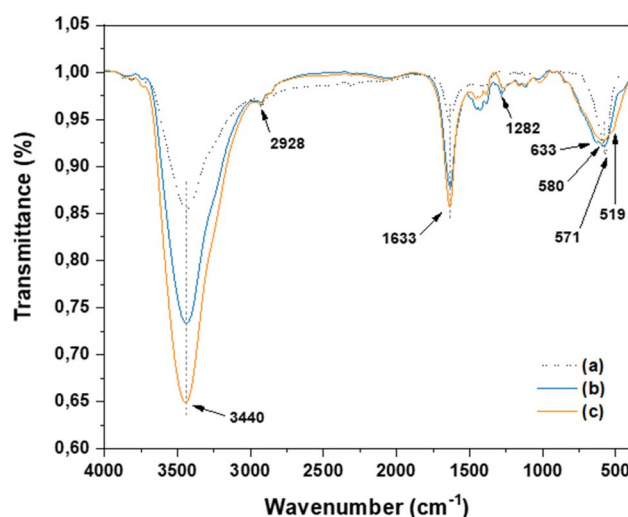
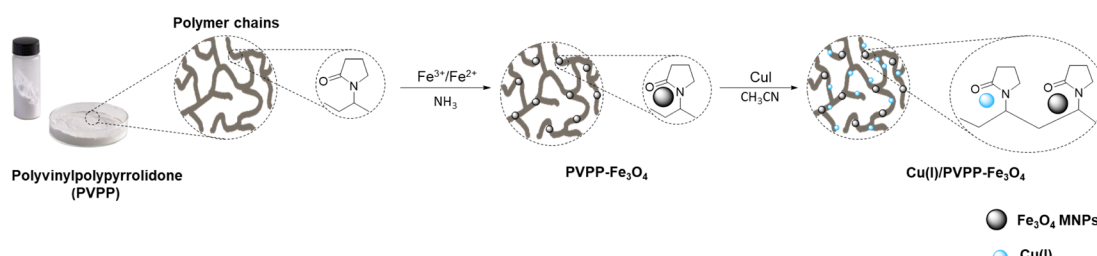


Fig. 1 FT-IR spectra of Fe<sub>3</sub>O<sub>4</sub> nanoparticles (a, black dash line), PVPP-Fe<sub>3</sub>O<sub>4</sub> (b, blue), and Cu(i)/PVPP-Fe<sub>3</sub>O<sub>4</sub> (c, orange) composite.



Scheme 1 Preparative route of Cu(i)/PVPP-Fe<sub>3</sub>O<sub>4</sub> composites.



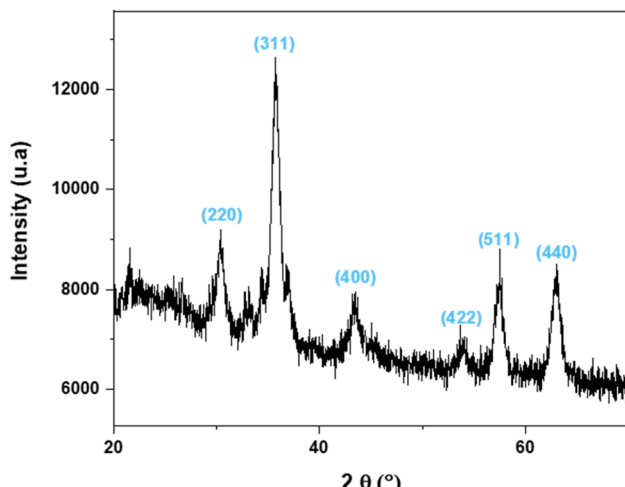


Fig. 2 XRD pattern of Cu(i)/PVPP-Fe<sub>3</sub>O<sub>4</sub> composite.

materials was characterized by FT-IR spectroscopy, X-ray diffraction, SEM, EDX, and AAS.

FT-IR spectra of the three samples, namely Fe<sub>3</sub>O<sub>4</sub> nanoparticles, PVPP-Fe<sub>3</sub>O<sub>4</sub>, and Cu(i)/PVPP-Fe<sub>3</sub>O<sub>4</sub> composites are shown in Fig. 1. The analysis of the spectrum of Fe<sub>3</sub>O<sub>4</sub> reveals the occurrence of absorption bands at 3440 and 580 cm<sup>-1</sup> that could be attributed to -OH and Fe-O stretching vibrations, respectively.<sup>20</sup> Shifts in the Fe-O band towards higher wave-numbers, changes in intensity, and a new band at 633 cm<sup>-1</sup> in

the PVPP-Fe<sub>3</sub>O<sub>4</sub> and Cu(i)/PVPP-Fe<sub>3</sub>O<sub>4</sub> spectra suggest coordination bonds and hydrogen bonding between the nanoparticles and PVPP. Both PVPP-Fe<sub>3</sub>O<sub>4</sub> and Cu(i)/PVPP-Fe<sub>3</sub>O<sub>4</sub> also show almost the same spectrum of the PVPP polymer, including C-H, C=O, and C-N vibration peaks at 2928, 1633, and 1282 cm<sup>-1</sup>, respectively. The Cu(i)-PVPP-Fe<sub>3</sub>O<sub>4</sub> spectrum shows an additional peak at 519 cm<sup>-1</sup>, indicating Cu-O vibrations and suggesting potential covalent bonding.<sup>9,10,20</sup> These interactions, along with electrostatic interactions and van der Waals forces, confirm the successful attachment of Fe<sub>3</sub>O<sub>4</sub> nanoparticles and Cu(i) ions to the PVPP polymer.

The analysis of the crystallinity and phase composition of the Cu(i)/PVPP-Fe<sub>3</sub>O<sub>4</sub> composite was carried out by XRD (see Fig. 2). The diffraction peaks at 2θ values of 30.39, 35.72, 43.42, 53.95, 57.52 and 63.04° correspond to the diffraction of the (220), (311), (400), (422), (511) and (440) planes of the cubic structure of the Fe<sub>3</sub>O<sub>4</sub> phase (JCPDS: 19-629).<sup>20</sup> The average diameter of the Fe<sub>3</sub>O<sub>4</sub> nanoparticles was estimated to be 8.6 nm according to Scherrer's formula.<sup>31</sup> Furthermore, the XRD analysis of the resultant composite confirms the formation of the crystal structure of the magnetic Fe<sub>3</sub>O<sub>4</sub> within the PVPP matrix by using the *in situ* method. Notably, no discernible signals corresponding to copper ions were detected in the XRD pattern. This absence of copper signals suggests that the copper species are likely dispersed on the support in the ionic form.

Surface morphological studies of PVPP-Fe<sub>3</sub>O<sub>4</sub> and Cu(i)/PVPP-Fe<sub>3</sub>O<sub>4</sub> composites were explored by the SEM technique (Fig. 3). The results of the SEM analysis reveal that the Fe<sub>3</sub>O<sub>4</sub>

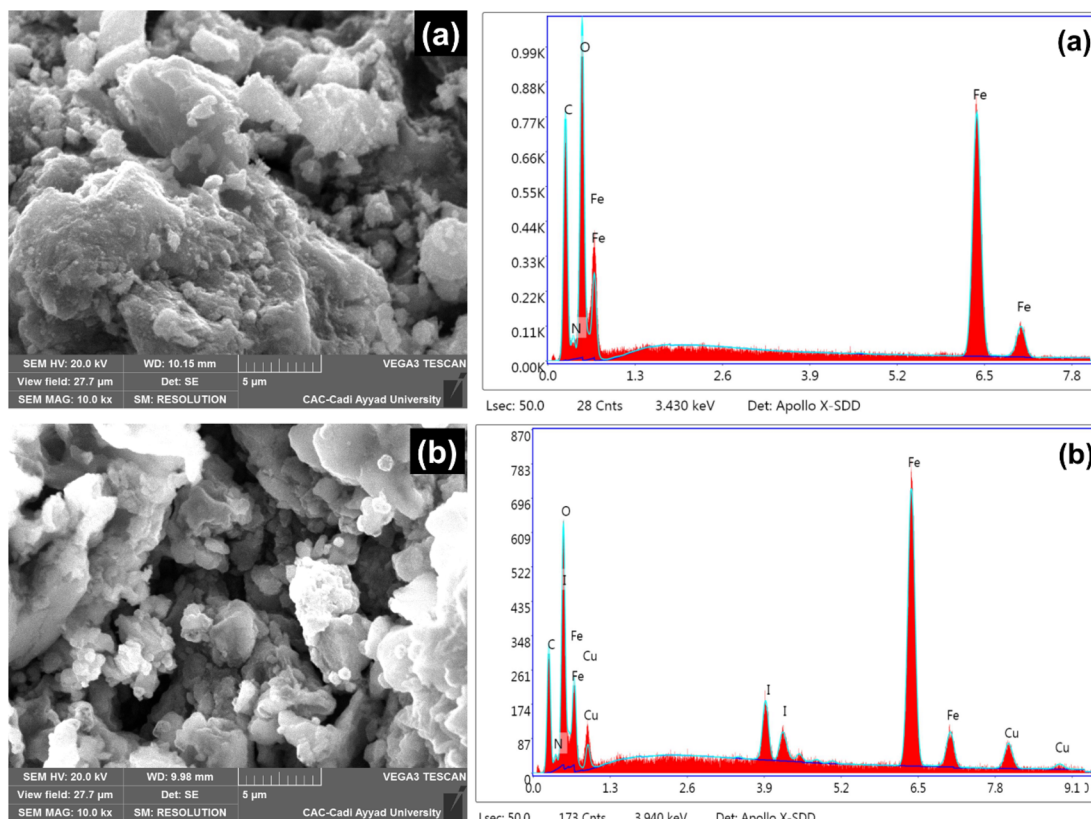
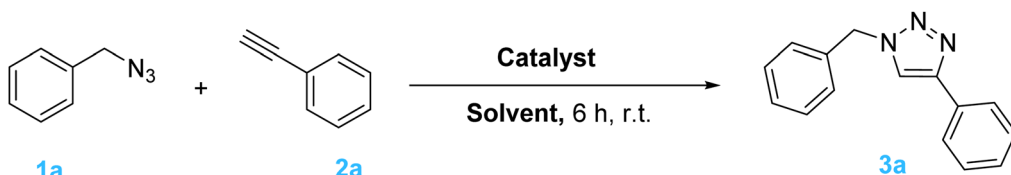


Fig. 3 SEM images and EDX spectra of PVPP-Fe<sub>3</sub>O<sub>4</sub> (a) and Cu(i)/PVPP-Fe<sub>3</sub>O<sub>4</sub> (b) composites.



**Table 1** Optimization of the reaction conditions for the azide–alkyne cycloaddition reaction of benzyl azide and phenylacetylene in the presence of Cu(i)/PVPP-Fe<sub>3</sub>O<sub>4</sub><sup>a</sup>



Entry	Catalyst	Catalyst amount (mol%)	Solvent	Yield <sup>b</sup> (%)
1	Cu(i)/PVPP-Fe <sub>3</sub> O <sub>4</sub>	0.3	H <sub>2</sub> O	97
2	Cu(i)/PVPP-Fe <sub>3</sub> O <sub>4</sub>	0.2	H <sub>2</sub> O	92
3	Cu(i)/PVPP-Fe <sub>3</sub> O <sub>4</sub>	0.1	H <sub>2</sub> O	65
4	Cu(i)/PVPP-Fe <sub>3</sub> O <sub>4</sub>	0.2	Toluene	54
5	Cu(i)/PVPP-Fe <sub>3</sub> O <sub>4</sub>	0.2	Ethanol	47
6	Cu(i)/PVPP-Fe <sub>3</sub> O <sub>4</sub>	0.2	Toluene/H <sub>2</sub> O (1 : 1 v/v)	41
7	Cu(i)/PVPP-Fe <sub>3</sub> O <sub>4</sub>	0.2	Ethanol/H <sub>2</sub> O (1 : 1 v/v)	51
8	PVPP-Fe <sub>3</sub> O <sub>4</sub>	0.2	H <sub>2</sub> O	—
9	PVPP	0.2	H <sub>2</sub> O	—
10	CuI	0.2	H <sub>2</sub> O	93

<sup>a</sup> Reaction conditions: 0.376 mmol of benzaldehyde, 0.313 mmol of phenylacetylene, catalyst, and solvent. <sup>b</sup> Isolated yield of the 1,4-regioisomer 3a.

nanoparticles and copper(i) ions were properly dispersed within the PVPP matrix, a feature that was directly related to the good complexation between the desired metals and PVPP functional groups. The elemental composition of PVPP-Fe<sub>3</sub>O<sub>4</sub> and Cu(i)/PVPP-Fe<sub>3</sub>O<sub>4</sub> composites are also presented in Fig. 3. The EDX spectrum showcases the presence of the desired elements in the investigated materials. The amount of copper was found to be 3.31 wt% as determined by Atomic Absorption Spectroscopy (AAS).

#### Catalytic study of Cu(i)/PVPP-Fe<sub>3</sub>O<sub>4</sub>

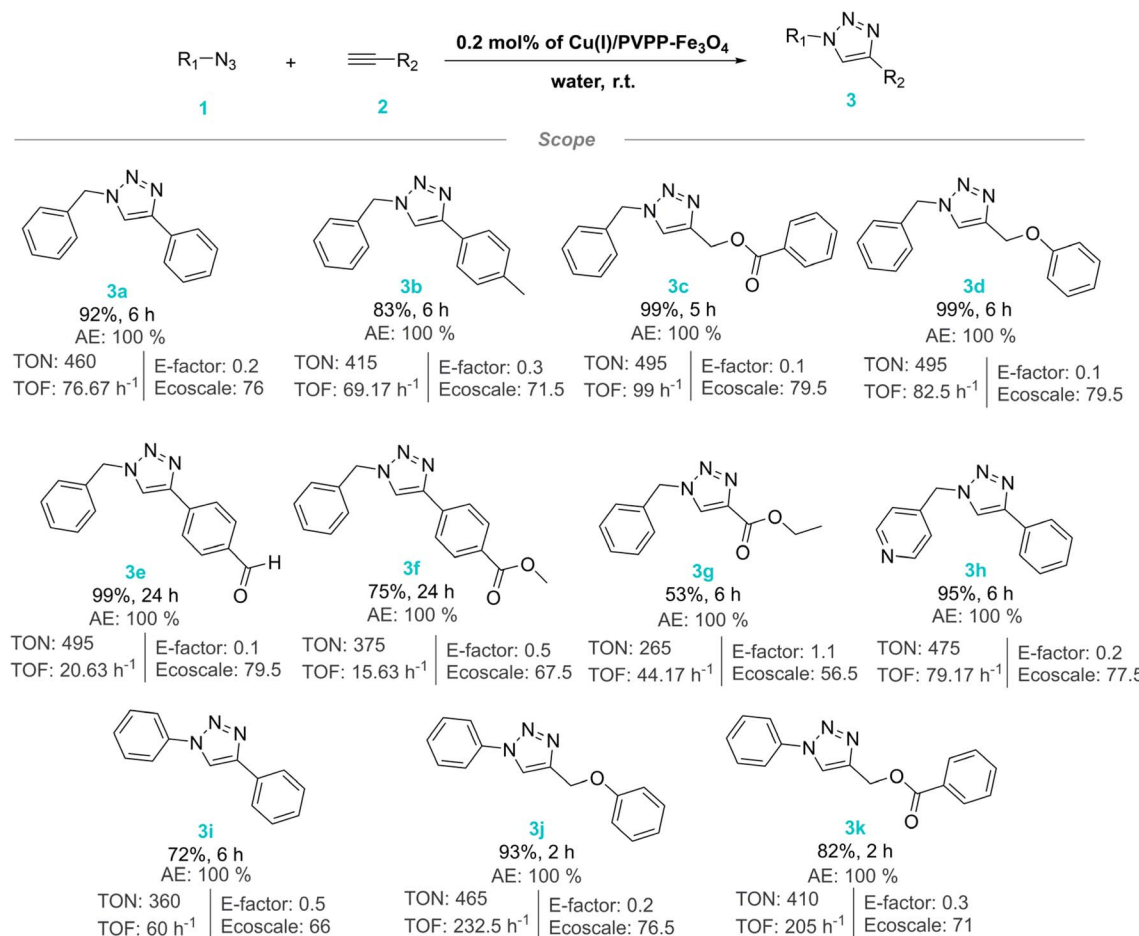
To study the catalytic performance of the prepared catalyst in CuAAC, the copper-catalyzed benzyl azide (1a) and phenylacetylene (2a) cycloaddition reaction was used as model reaction. This investigation involved the systematic examination of different solvents and varying amounts of catalysts. The catalytic results are summarized in Table 1. The optimum reaction conditions correspond to the use of 0.2 mol% of catalyst in water as solvent at room temperature (entries 1–7). The use of organic solvents like ethanol and toluene or a decrease in the amount of catalyst until 0.1 mol% result in a decrease in its catalytic activity. Moreover, a negligible formation of the product (entries 8–10) was observed when employing only PVPP or PVPP-Fe<sub>3</sub>O<sub>4</sub> materials instead of using only CuI. This result supports the essential role of copper in the Cu(i)/PVPP-Fe<sub>3</sub>O<sub>4</sub> composite to obtain the final 1,2,3-triazole (3a).

After optimizing the reaction conditions, the CuAAC reaction was studied for substrates scope using diverse organic azides and terminal alkynes (Scheme 2). Overall, the reactions proceeded successfully with all employed reagents, whether they contain electron-donating or electron-withdrawing substituents. This resulted in the formation of the respective 1,4-disubstituted-1,2,3-triazole derivatives in excellent yields with

good turnover numbers (TON) ranging from 495 to 265 except for 3g. Furthermore, most of the synthesized products were obtained within a short time and without additional purification by using conventional methods. Specifically, we found that compounds 3j and 3k were obtained within just 2 hours, whereas 3e and 3f required 24 hours. The other compounds were typically obtained within 5 to 6 hours. The variation in reaction times could be attributed to the electronic effect of the substituents on alkynes and the reactivity of azides, as well as the overall molecular environment and steric factors. For instance, the compound 3j contains an electron-donating group, namely phenoxyethyl, which increases the electron density on the alkyne. This makes the copper–acetylide complex more nucleophilic and reactive towards the electrophilic azide, resulting in shorter reaction time. Interestingly, the compound 3k also reacts quickly within 2 hours, despite having an electron-withdrawing at benzoate group. This could be due to the overall electronic environment created by the phenyl group, which might mitigate the electron-withdrawing effect of the benzoate. Additionally, the steric factors and specific interactions with the copper catalyst could facilitate a faster reaction. In contrast, compounds 3c and 3d exhibit intermediate reaction times. The benzyl group, while slightly electron-donating, introduces some steric hindrance that might slow down the reaction compared to less hindered systems. The compounds 3e and 3f have electron-withdrawing groups, which reduce the electron density on the alkyne, making the copper–acetylide complex more electrophilic and resulting in longer reaction times as the attack of the azide is less effective.

To evaluate the sustainability of the catalytic system under study, three sustainability metrics, namely Atom Economy (AE), E-factor, and EcoScale were applied to the CuAAC as shown in Scheme 2.<sup>32–34</sup> The developed CuAAC process using Cu(i)/PVPP-





**Scheme 2** Scope of azide–alkyne cycloaddition reactions catalyzed by the Cu(I)/PVPP-Fe<sub>3</sub>O<sub>4</sub> catalyst to afford the 1,4-disubstituted-1,2,3-triazole products after recrystallization. Abbreviations: AE = atom economy; TON = turnover number; TOF = turnover frequency (TON/time).

Fe<sub>3</sub>O<sub>4</sub> exhibits high atom economy of all products with minimum to moderate waste production (E-factor: 0.1–1.1) and moderate to good sustainability (EcoScale: 79.5–56.5) owing to its safety profile and convenient workup.

The reusability of the catalyst is a key issue of heterogeneous catalysis. So, the potential for recovering the Cu(I)/PVPP-Fe<sub>3</sub>O<sub>4</sub> catalyst was explored (Fig. 4). After the end of the model reaction, the reaction mixture was diluted using dichloromethane, and the

catalyst was effortlessly recovered using an external magnet. Subsequently, the recovered catalyst was washed with dichloromethane and water. Then, the dried catalyst was used in a next fresh model CuAAC reaction. The results showed that the magnetically separable catalyst could be reused until five consecutive times with a slight to moderate loss of its catalytic activity.

The kinetic study of the fresh and the first reused Cu(I)/PVPP-Fe<sub>3</sub>O<sub>4</sub> catalyst was also carried out, and the results obtained are

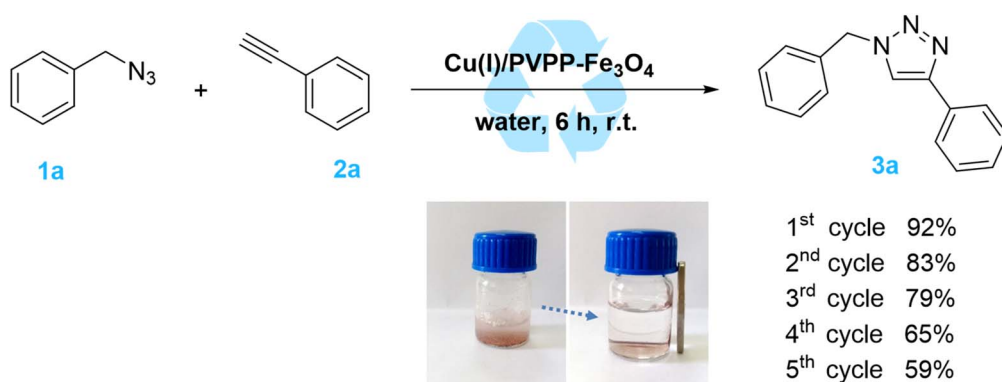


**Fig. 4** Reusing the Cu(I)/PVPP-Fe<sub>3</sub>O<sub>4</sub> catalyst in the CuAAC reaction between benzyl azide and phenylacetylene.

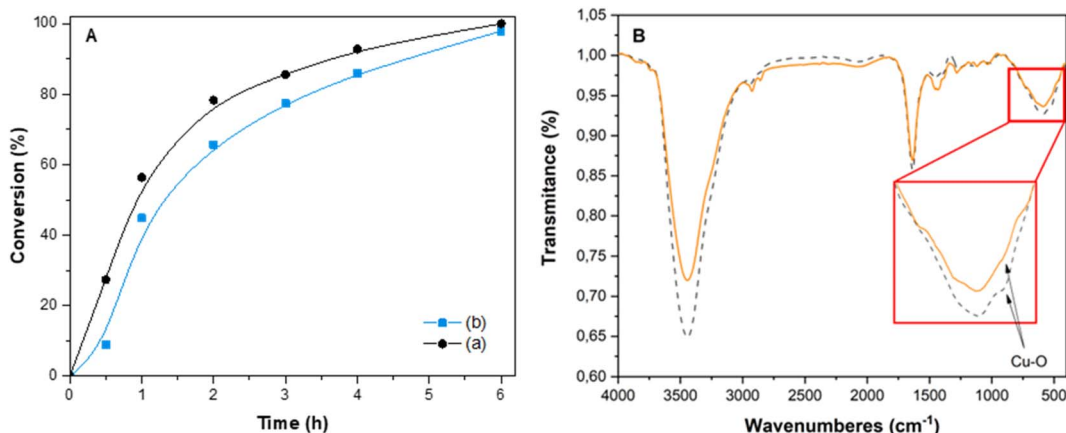


Fig. 5 (A) Reaction profile of the CuAAC reaction between benzyl azide and phenylacetylene catalyzed by the fresh catalyst (a) and first reused catalyst (b). (B) FT-IR spectra of the fresh (dashed trace) and reused catalyst (red trace) after five runs.

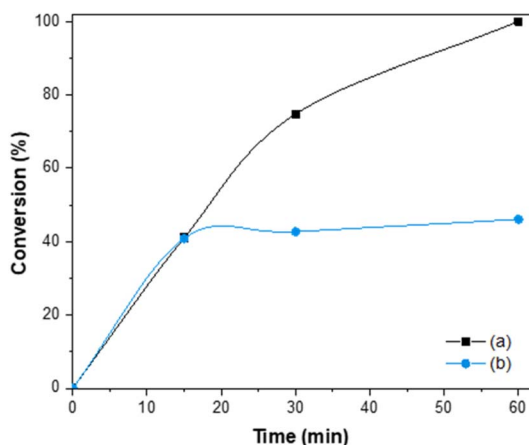


Fig. 6 Reaction profile of the model reaction at 60 °C (a) and that of the CuAAC reaction after removal of the Cu(i)/PVPP-Fe<sub>3</sub>O<sub>4</sub> catalyst by hot filtration at 15 min (b).

shown in Fig. 5. When the catalyst was reused in a second cycle, no significant decrease in its activity was observed during the catalytic reaction monitored by GC analysis. This result suggests that the prepared catalyst remains stable, while its significant loss, during the recovery process, could be attributed to the extraction process of 1,2,3-triazole products. The fact that the peak positions in the FT-IR spectra of the fresh and used catalyst remained unaltered after five runs, confirms that the structure of the recovered catalyst did not undergo any significant change compared to the one of the fresh catalyst (Fig. 5).

A leaching experiment was also performed to check the stability of the prepared catalyst. In this respect, the hot filtration test for the model reaction between benzyl azide and phenylacetylene was carried out at 60 °C, and the obtained results are illustrated by Fig. 6. After the removal of the catalyst *via* hot filtration at approximately 40%, the reaction was stopped, and the yield of the product did not significantly increase further even after 45 min under the same conditions. These results suggest that the Cu(i)/PVPP-Fe<sub>3</sub>O<sub>4</sub> composite is an

efficient, stable, and magnetic reusable heterogeneous catalyst for the CuAAC click chemistry reaction, with residual copper particles, less than 0.6 ppm, in the final 1,2,3-triazole product as determined by the analysis using AAS.

To prove the efficiency of the present process for the synthesis of 1,4-disubstituted-1,2,3-triazole compounds, the model reaction was compared to the previously reported data in the literature (Table S1†). The results of this catalytic process align well with those from the literature in terms of cost-effectiveness, yields, and environmentally friendly reaction conditions. Furthermore, our catalytic system could also be performed in a one-pot system as shown in Fig. 7. The kinetic study of the one-pot process revealed that the reaction could be used for the *in situ* formation of the azide derivative from the corresponding halogenated precursors and sodium azide, to successively react with the acetylene resulting in the desired 1,4-disubstituted-1,2,3-triazole compound. This catalytic system is considered a cost-effective and ecobenign process, as it avoids

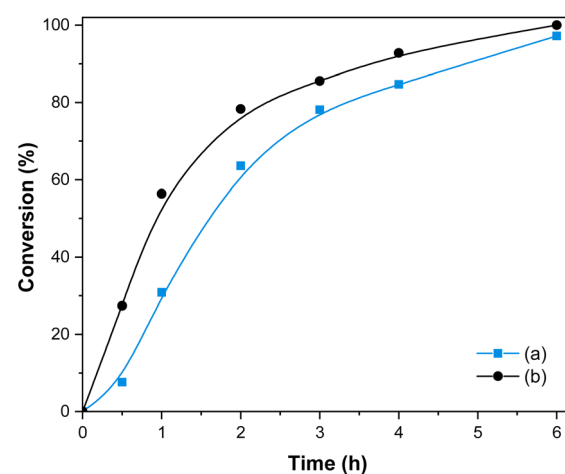
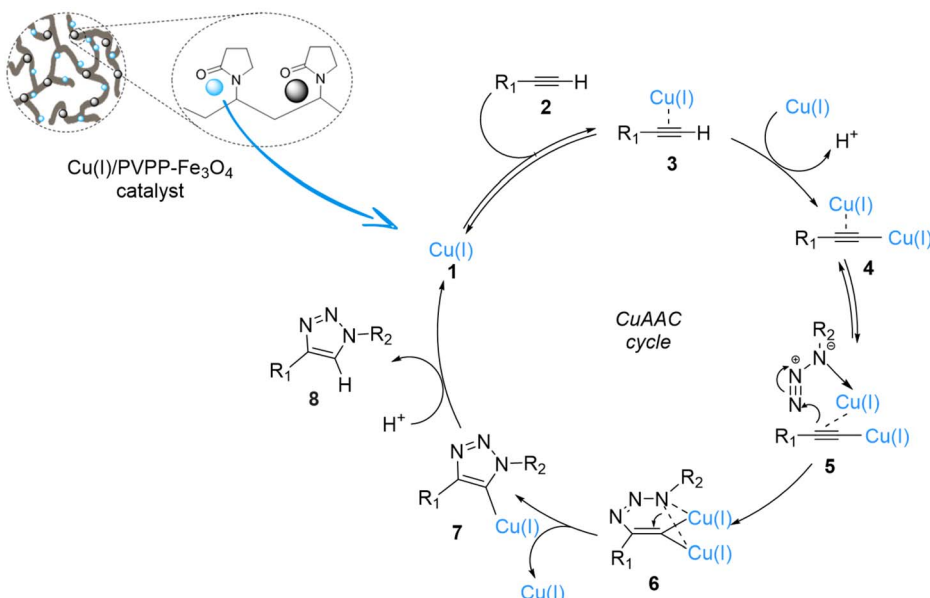


Fig. 7 Reaction profile of the CuAAC reaction when benzyl azide was formed *in situ* from benzyl bromide and sodium azide (a), and its comparison with the reaction initiated directly from benzyl azide (b).



Scheme 3 Proposed mechanism for the azide–alkyne cycloaddition reaction catalyzed by the Cu(I)/PVPP-Fe<sub>3</sub>O<sub>4</sub> catalyst.

costly separation and purification of intermediates, while requiring lower process investment and energy consumption.

#### Plausible mechanism

The mechanistic pathways suggested for the synthesis of 1,4-disubstituted-1,2,3-triazole compounds in the presence of Cu(I)/PVPP-Fe<sub>3</sub>O<sub>4</sub> were proposed according to literature data<sup>35,36</sup> (Scheme 3). The intermediate 4 is formed in the first step when the active copper(I) species coordinates with the terminal alkyne. Then, the copper–acetylide undergoes a reaction with the azide reagent (5), resulting in the formation of the intermediate 6. In the last step, the copper triazolide (7) selectively attacks a proton to yield the regioselective formation of the 1,4-disubstituted-1,2,3-triazole product (8).

## Conclusions

To summarize, we have prepared a new magnetic composite catalyst by incorporating Cu(I) into the cross-linked PVPP-Fe<sub>3</sub>O<sub>4</sub> composite that allows an efficient separation and recovery from the final 1,2,3-triazoles. This catalyst exhibits good catalytic activity in azide–alkyne 1,3-dipolar cycloaddition reactions between organic azides and terminal alkynes in water at room temperature together with low copper loadings to the selective formation of the corresponding 1,4-disubstituted-1,2,3-triazoles, with good to excellent yields and excellent atom economy. Moreover, the prepared catalyst could be easily separated and recovered from the reaction mixture with the application of an external magnet and reused for four additional runs. The remarkable aspects of this catalytic process include the use of greener conditions, straightforward operation, simple product isolation, and recyclability of the catalyst, all these features point to the development of the sustainable side of CuAAC click chemistry process.

## Experimental section

### Materials and methods

All chemicals and solvents were used as purchased from commercial sources (Sigma-Aldrich, Fluka, and Alfa-Aesar) without further purification. The organic azides were synthesized according to the literature.<sup>9</sup> The FT-IR spectra were performed on a FT-IR Nicolet 5700 spectrophotometer. The X-ray diffraction (XRD) analysis was determined on a proprietary X-ray powder diffractometer (Empyrean PANalytical). This experiment was conducted using a copper anticathode at a voltage of 40 kV, with incident radiation from a Cu K $\alpha$  source ( $\lambda = 1.5418 \text{ \AA}$ ). The Scanning Electron Microscopy (SEM) analysis was carried out with a VEGA3 TESCAN microscope, while Energy-dispersive X-ray (EDX) analysis was done with a high-resolution JEOL Field Emission Gun-Scanning Electron Microscope (FEG-SEM). Copper contents in the synthesized materials were determined using Atomic Absorption Spectroscopy (AAS) with the Aurora AI800 instrument. The purity of the products was assessed through TLC (thin-layer chromatography) using commercial aluminum-backed silica gel plates (Merck Kieselgel 60 F254). The plates were examined under UV light at a wavelength of 254 nm. The melting points were measured by means of an Electrothermal IA9100 electrothermal melting point apparatus, with the use of capillary tubes. The NMR spectra were registered by using a BRUCKER AC-400 MHz spectrometer in CDCl<sub>3</sub> as the solvent, with TMS serving as the internal standard. High-resolution mass spectra (HR-MS) were recorded at the mass spectrometry service of the University of Valencia, either in the EI mode with 70 eV or in the FAB mode. Kinetic experiments were conducted by the Trace 1300 Thermo Scientific gas chromatograph equipped with a TG-5MS column (30 m  $\times$  0.25 mm  $\times$  0.25  $\mu\text{m}$ ) and a Flame Ionization Detector.



### Synthesis of the PVPP- $\text{Fe}_3\text{O}_4$ nanocomposite

1.3 g of  $\text{FeCl}_3 \cdot 6\text{H}_2\text{O}$  and 0.63 g of  $\text{FeCl}_2 \cdot 4\text{H}_2\text{O}$  were dissolved in 35 mL of water in a round bottom flask at room temperature in the open air. Then, 1 g of PVPP was added to the solution mixture and kept for another 1 hour under the same conditions. After that, 15 mL of 25% ammonia solution was added dropwise to the resulting reaction mixture, and the temperature was slowly increased to 80 °C under continuous stirring for 2 hours. The resulting black-colored precipitate was picked by using an external magnet, washed several times with water until  $\text{pH} = 7$ , and then with ethanol. The solid PVPP- $\text{Fe}_3\text{O}_4$  nanocomposite was dried in a vacuum.

### Preparation of the $\text{Cu}(\text{i})/\text{PVPP-Fe}_3\text{O}_4$ catalyst

200 mg of PVPP- $\text{Fe}_3\text{O}_4$  was dispersed in a previously prepared solution of copper(i) iodide (50 mg) in acetonitrile (5 mL) and ultra-sonicated for 30 min at room temperature. Then, the mixture was transferred to a mechanical stirrer for another 16 hours at room temperature. The resulting material was picked by means of an external magnetic field, rinsed multiple times with acetonitrile and water, and then allowed to dry under vacuum overnight.

### Synthesis of 1,2,3-triazoles

0.376 mmol of azide derivative, 0.313 mmol of alkyne derivative, and 5 mg of  $\text{Cu}(\text{i})/\text{PVPP-Fe}_3\text{O}_4$  catalyst (0.2 mol% of copper) were introduced in a round bottom flask, and 3 mL of water was added. The mixture was stirred using a mechanical stirrer at room temperature. Then, the reaction mixture was monitored using TLC with an ethyl acetate/hexane eluent. Once the reaction was completed, the resulting mixture was diluted with dichloromethane. The catalyst was then separated using a magnet, washed multiple times with dichloromethane, followed by water, and finally dried under vacuum. In the next step, the corresponding product was extracted with dichloromethane, subsequently dried by anhydrous  $\text{MgSO}_4$  and then evaporated under reduced pressure to give the final product. The resulting compound was purified by recrystallization from a dichloromethane/hexane solvent mixture.

Table 2 Calculation of the atom economy of our process

Product	Molar mass of all reactants (g mol <sup>-1</sup> )	Molar mass of desired product (g mol <sup>-1</sup> )	AE (%)
3a	236.1188	236.1177	100
3b	250.1339	250.1339	100
3c	294.1237	294.1241	100
3d	266.1288	266.1289	100
3e	264.1137	264.1134	100
3f	294.1237	294.1242	100
3g	232.1086	232.1087	100
3h	236.1062	237.1132	100
3i	222.1031	222.1029	100
3j	252.1130	252.1129	100
3k	280.1080	280.1080	100

Table 3 Calculation of the E-factor of our process

Product	Amount of azide (mg)	Amount of alkyne (mg)	Amount of product (mg)	E-factor
3a	50	31.96	67.75	0.2
3b	50	36.35	64.76	0.3
3c	50	50.13	90.89	0.1
3d	50	41.36	82.21	0.1
3e	50	40.73	81.58	0.1
3f	50	50.13	68.86	0.5
3g	50	30.7	38.36	1.1
3h	50.43	31.96	70.25	0.2
3i	44.79	31.96	49.86	0.5
3j	44.79	41.36	73.15	0.2
3k	44.79	50.13	71.68	0.3

### Calculation of atom economy (AE), E-factor, and EcoScale values

AE is a factor to measure the efficiency of a chemical reaction which is defined by the following expression:<sup>32</sup>

$$\text{AE} = \frac{\text{molar mass of desired product}}{\text{molar mass of all reactants}} \times 100$$

This parameter indicates the proportion of reactant atoms that ends up in the desired product. A high value of AE is the sign of a more efficient and environmentally friendly reaction with most of reactant atoms incorporated into the desired product. In present case, the values of AE are listed in Table 2.

The E-factor is parameter to measure the environmental impact of a chemical process which obeys to the following expression:<sup>22</sup>

$$\text{E-factor} = \frac{\text{mass of total waste}}{\text{mass of product}}$$

It indicates the amount of waste generated per unit of product. A low value of the E-factor is a sign of a greener and more efficient process with less waste, while a high one highlights less efficient process with more waste. As all the solvents and the catalyst can be reused, only the unreacted reagents are considered for the total mass of waste, and the E-factor will be calculated using the following formula:

$$\text{E-factor} =$$

$$\frac{\text{total amount of reactants} - \text{amount of final product}}{\text{mass of product}}$$

The values of the E-factor in the present study are listed in Table 3.

EcoScale is a parameter to measure the greenness of a chemical process, considering factors such as yield, cost, safety, and environmental impact. The EcoScale is calculated using a scoring system where the ideal score is 100, with points deducted for non-ideal conditions and practices. It is calculated using the following formula<sup>34</sup>



Table 4 Calculation of the EcoScale of our process

Product	Penalty										
	3a	3b	3c	3d	3e	3f	3g	3h	3i	3j	3k
1 <b>Yield</b>	4	8.5	0.5	0.5	0.5	12.5	23.5	2.5	14	3.5	9
2 <b>Price of reaction components (to obtain 10 mmol of end product)</b>											
Cu(i)/PVPP-Fe <sub>3</sub> O <sub>4</sub> (0.2 mol%)	0	0	0	0	0	0	0	0	0	0	0
H <sub>2</sub> O	0	0	0	0	0	0	0	0	0	0	0
3 <b>Safety</b>											
Azide	5	5	5	5	5	5	5	5	5	5	5
Alkyne	5	5	5	5	5	5	5	5	5	5	5
Cu(i)/PVPP-Fe <sub>3</sub> O <sub>4</sub>	5	5	5	5	5	5	5	5	5	5	5
H <sub>2</sub> O	0	0	0	0	0	0	0	0	0	0	0
4 <b>Technical setup</b>											
Common glass ware stirring	0	0	0	0	0	0	0	0	0	0	0
5 <b>Temperature/time</b>											
Room temperature ≤24 h	1	1	1	1	1	1	1	1	1	1	1
6 <b>Workup and purification</b>											
Liquid–liquid extraction	3	3	3	3	3	3	3	3	3	3	3
Crystallization and filtration	1	1	1	1	1	1	1	1	1	1	1
Penalty points total	24	28.5	20.5	20.5	20.5	32.5	43.5	22.5	34	23.5	29
<b>EcoScale</b>	76	71.5	79.5	79.5	79.5	67.5	56.5	77.5	66	76.5	71

$$\text{EcoScale} = 100 - \text{sum of individual penalties}$$

High EcoScale scores indicates a greener, more sustainable chemical process, while low ones highlight areas for improvement environmental and safety aspects.

The EcoScale of our process was calculated based on the penalties reported in the literature,<sup>34</sup> as presented in Table 4.

### Kinetic experiments

In the experimental procedure, stoichiometric amounts of reagents and identical amounts of catalyst and solvent were introduced into a round bottom flask. Then, the mixtures underwent monitoring by using Gas Chromatography (GC). To ensure that the experiments were suitable for GC analysis, the samples were extracted at specified time intervals, using the same volume of diethyl ether. After this, they were analyzed by gas chromatograph using helium as carrier gas at a constant flow rate of 0.2 mL min<sup>-1</sup> and setting the system temperature of the injector (in mode split flow), colon, and detector at 200 °C within 6 min. Finally, the conversion of the reaction *vs.* time was calculated from the concentration of alkyne through the following equation:

$$\text{Conversion} = \frac{C_0 - C_t}{C_0} \times 100$$

where  $C_0$  and  $C_t$  are the concentrations of alkyne at  $t = 0$  and at time  $t$  of the reaction, respectively.

### Data availability

The data supporting of this article have been included as part of the ESI.†

### Author contributions

All authors have contributed equally to the preparation of this submission.

### Conflicts of interest

The authors declare no conflict of interest and no competing financial interest.

### Acknowledgements

University Cadi Ayyad (Morocco) and University of Valencia (Spain) are acknowledged for the facilities and support provided to this research program.

### References

- 1 S. Zhao, J. Liu, Z. Lv, G. Zhang and Z. Xu, *Eur. J. Med. Chem.*, 2023, **251**, 115254.
- 2 R. Huisgen, *Proc. Chem. Soc.*, 1961, 357–396.
- 3 H. C. Kolb, M. G. Finn and K. B. Sharpless, *Angew Chem., Int. Ed.*, 2001, **40**, 2004–2021.
- 4 V. V. Rostovtsev, L. G. Green, V. V. Fokin and K. B. Sharpless, *Angew Chem., Int. Ed.*, 2002, **41**, 2596–2599.
- 5 C. W. Tornøe, C. Christensen and M. Meldal, *J. Org. Chem.*, 2002, **67**, 3057–3064.
- 6 S. Asadi, B. Bahramian, A. Dehno Khalaji, V. Mirdarvatan, M. Bakherad and A. Rezaeifard, *Cellulose*, 2024, **31**, 3497–3516.
- 7 N. Aflak, H. Ben El Ayouchia, L. Bahsis, H. Anane, M. Julve and S.-E. Stiriba, *Int. J. Mol. Sci.*, 2022, **23**, 2383.



8 S. Stiriba, N. Aflak, E. M. El Mouchtari, H. Ben El Ayouchia, S. Rafqah, H. Anane and M. Julve, *Appl. Organomet. Chem.*, 2023, **37**(8), e7175.

9 N. Aflak, H. Ben El Ayouchia, L. Bahsis, E. M. El Mouchtari, M. Julve, S. Rafqah, H. Anane and S.-E. Stiriba, *Front. Chem.*, 2019, **7**, 81.

10 N. Aflak, H. Ben El Ayouchia, L. Bahsis, H. Anane, R. Laamari, A. Pascual-Alvarez, D. Armentano and S.-E. Stiriba, *Polyhedron*, 2019, **170**, 630–638.

11 N. Aflak, L. El Mersly, H. Ben El Ayouchia, S. Rafqah, H. Anane, M. Julve and S.-E. Stiriba, *J. Coord. Chem.*, 2022, **75**, 2346–2358.

12 S. Kalhor, H. Sepehrmansourie, M. Zarei, M. A. Zolfigol and H. Shi, *Inorg. Chem.*, 2024, **63**, 4898–4914.

13 S. Fu, G. Liu, S. Liu, Z. Gao, S. Tao, Y. Peng, N. Xin, X. Huang and G. Yang, *Mol. Catal.*, 2024, **562**, 114185.

14 J. Pandey, B. D. Singh, H. Khanam, B. Tiwari, T. Azaz and R. Singh, *Int. J. Biol. Macromol.*, 2024, **255**, 128098.

15 S. Kasana, V. Nigam, S. Singh, B. Das Kurmi and P. Patel, *Chem. Biodiversity*, 2024, e202400109.

16 M. Ashrafi, M. Amini and F. Seidi, *Langmuir*, 2024, **40**, 5195–5204.

17 O. Jennah, R. Beniaffa, C. Lozach, D. Jardel, F. Molton, C. Duboc, T. Buffeteau, A. El Kadib, D. Lastécouères, M. Lahcini and J. Vincent, *Adv. Synth. Catal.*, 2018, **360**, 4615–4624.

18 S. H. Gebre, *Appl. Nanosci.*, 2023, **13**, 15–63.

19 Z. B. Shifrina and L. M. Bronstein, *Front. Chem.*, 2018, **6**, 298.

20 N. Aflak, E. M. El Mouchtari, H. Ben El Ayouchia, H. Anane, S. Rafqah, M. Julve and S.-E. Stiriba, *Catalysts*, 2022, **12**, 1244.

21 I. Ahmad, M. A. Aftab, A. Fatima, S. D. Mekkey, S. Melhi and S. Ikram, *Coord. Chem. Rev.*, 2024, **514**, 215904.

22 S.-W. Chen, Z.-C. Zhang, N.-N. Zhai, C.-M. Zhong and S. Lee, *Tetrahedron*, 2015, **71**, 648–653.

23 J. Zhao, Y. Gui, Y. Liu, G. Wang, H. Zhang, Y. Sun and S. Fang, *Catal. Lett.*, 2017, **147**, 1127–1132.

24 K. A. Bezlepkinsa, I. I. Belikova, V. A. Aristova, K. S. Klokov, S. N. Ardabevskaia, A. Y. Pereyaslavtsev, D. A. Migulin and S. A. Milenin, *React. Chem. Eng.*, 2023, **9**, 448–460.

25 R. Singh, G. Singh, N. George, G. Singh, S. Gupta, H. Singh, G. Kaur and J. Singh, *Catalysts*, 2023, **13**, 130.

26 Z. Lei, H. T. Ang and J. Wu, *Org. Process Res. Dev.*, 2024, **28**, 1355–1368.

27 S. Wang and C. Tian, *Int. J. Polym. Sci.*, 2016, **2016**, 1–7.

28 S. Khaksar, M. Tajbakhsh and M. Gholami, *C. R. Chim.*, 2014, **17**, 30–34.

29 M. Mokhtary, M. M. Lakouraj and M. R. Niaki, *Phosphorus, Sulfur Silicon Relat. Elem.*, 2012, **187**, 321–326.

30 L. Bahsis, M. El Himri, H. Ben El Ayouchia, H. Anane, E. Ablouh, M. Julve and S. Stiriba, *Macromol. Chem. Phys.*, 2019, **220**, 1900311.

31 B. D. Cullity and R. Smoluchowski, *Phys. Today*, 1957, **10**, 50.

32 B. Trost, *Science*, 1991, **254**, 1471–1477.

33 R. A. Sheldon, *Green Chem.*, 2007, **9**, 1273.

34 K. Van Aken, L. Strekowski and L. Patiny, *Beilstein J. Org. Chem.*, 2006, **2**(1), 3.

35 H. Ben El Ayouchia, L. Bahsis, H. Anane, L. R. Domingo and S.-E. Stiriba, *RSC Adv.*, 2018, **8**, 7670–7678.

36 B. T. Worrell, J. A. Malik and V. V. Fokin, *Science*, 2013, **340**, 457–460.